Heliyon 9 (2023) e20089

Contents lists available at ScienceDirect

Heliyon

journal homepage: www.cell.com/heliyon

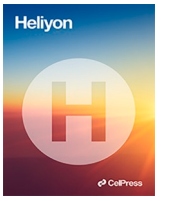

Curcumin-derived carbon-dots as a potential COVID-19 antiviral drug

Azzania Fibriani [a,e,*], Audrey Angelina Putri Taharuddin [a], Rebecca Stephanie [a], Nicholas Yamahoki [a], Jessica Laurelia [a], Popi Hadi Wisnuwardhani [b], Dian Fitria Agustiyanti [b], Marissa Angelina [c], Yana Rubiyana [b], Ratih Asmana Ningrum [b], Andri Wardiana [b], Ferry Iskandar [d,e,f], Fitri Aulia Permatasari [d,f,g], Ernawati Arifin Giri-Rachman [a,e]

[a] *School of Life Sciences and Technology, Bandung Institute of Technology, Bandung, 40132, Indonesia*
[b] *Research Center for Genetic Engineering, Indonesian National Research and Innovation Agency (BRIN), Cibinong, 16911, Indonesia*
[c] *Research Center for Pharmaceutical Ingredients and Traditional Medicine, Indonesian National Research and Innovation Agency (BRIN), Serpong, 15314, Indonesia*
[d] *Department of Physics, Faculty of Mathematics and Natural Sciences, Bandung Institute of Technology, Bandung, 40132, Indonesia*
[e] *Research Center for Nanoscience and Nanotechnology, Bandung Institute of Technology, Bandung, 40132, Indonesia*
[f] *Collaboration Research Center for Advanced Energy Materials, National Research and Innovation Agency - Bandung Institute of Technology, Bandung, 40132, West Java, Indonesia*
[g] *Research Center for Chemistry, National Research and Innovation Agency (BRIN), Kawasan Puspiptek, 15314, Banten, Indonesia*

ARTICLE INFO

Keywords:
Antiviral activity
Curcumin
Carbon-dots
Nucleocapsid
SARS-CoV-2

ABSTRACT

Even entering the third year of the COVID-19 pandemic, only a small number of COVID-19 antiviral drugs are approved. Curcumin has previously shown antiviral activity against SARS-CoV-2 nucleocapsid, but its poor bioavailability limits its clinical uses. Utilizing nanotechnology structures, curcumin-derived carbon-dots (cur-CDs) were synthesized to increase low bioavailability of curcumin. *In-silico* analyses were performed using molecular docking, inhibition of SARS-CoV-2 nucleocapsid C-terminal domain (N-CTD) and antiviral activity were assessed in dimer-based screening system (DBSS) and *in vitro* respectively. Curcumin bound with the N-CTD at $\Delta G = -7.6$ kcal/mol, however modifications into cur-CDs significantly improved the binding affinity and %interaction. Cur-CDs also significantly increased protection against SARS-CoV-2 in both DBSS and *in vitro* at MOI = 0.1. This study demonstrated the effect of post-infection treatment of curcumin and novel curcumin-derived carbon-dots on SARS-CoV-2 N-CTD dimerization. Further investigation on pre-infection and *in-vivo* treatment of curcumin and cur-CDs are required for a comprehensive understanding on the carbon-dots enhanced antiviral activity of curcumin against SARS-CoV-2.

Abbreviations: cur-CDs, curcumin-derived carbon-dots; N-CTD, C-terminal domain of SARS-CoV-2 nucleocapsid.

* Corresponding author. Labtek XI, Jl. Ganeca No.10, Lb. Siliwangi, Coblong, Bandung, West Java, 40132, Indonesia.
E-mail addresses: afibriani@itb.ac.id (A. Fibriani), audreytaharuddin@gmail.com (A.A.P. Taharuddin), rebecca.stephanie.21@gmail.com (R. Stephanie), nicholasyamahoki@gmail.com (N. Yamahoki), jessicalaurelia07@gmail.com (J. Laurelia), popi002@brin.go.id (P.H. Wisnuwardhani), dian023@brin.go.id (D.F. Agustiyanti), mari011@brin.go.id (M. Angelina), yana006@brin.go.id (Y. Rubiyana), rati007@brin.go.id (R.A. Ningrum), andr027@brin.go.id (A. Wardiana), ferry@fi.itb.ac.id (F. Iskandar), f.aulia.p@gmail.com (F.A. Permatasari), erna@sith.itb.ac.id (E.A. Giri-Rachman).

https://doi.org/10.1016/j.heliyon.2023.e20089
Received 11 June 2023; Received in revised form 8 September 2023; Accepted 11 September 2023
Available online 12 September 2023

1. Introduction

The COVID-19 pandemic has caused more than 650 million cases and more than 6 million deaths globally, as of the end of January 2023 [1]. Although showing unprecedented speed in its development and distribution, COVID-19 vaccines are still unavailable to a large fraction of the global population and cannot serve as a preventive means for patients with high health risks. The possibility of partial resistance of the virus against vaccines due to mutations also put the development of antiviral drugs in constant relevance [2,3]. Despite this, as of May 2023, the United States Food and Drug Administration (FDA) has only approved four antiviral drugs for COVID-19 treatments: tocilizumab (Actemra), remdesivir (Veklury), baricitinib (Olumiant), and nirmatrelvir-ritonavir (Paxlovid) [4].

For its central role in facilitating viral replication and particle assembly, the nucleocapsid phosphoprotein has been the target of many preclinical and clinical drugs. The nucleocapsid primarily protects the viral genome and maintains reliable viral replication by forming a helical ribonucleoprotein complex with the viral RNA. Due to the highly conserved nature of the nucleocapsid, an antiviral drug targeting the nucleocapsid may be a promising prophylactic strategy and a solution for variants with reduced response to vaccines [5–7].

Curcumin, with molecular structure shown in Fig. 1, is the main phytochemical found in *Curcuma longa* (turmeric) and is primarily responsible for the anti-inflammatory, antioxidant, antiseptic, analgesic, antimicrobial (such as antibacterial, antifungal, antiviral, antimalarial) and anticancer properties of turmeric. Turmeric is widely cultivated in warmer climates and is widely consumed as a traditional herbal beverage in Indonesia for its immune-boosting properties [8–11].

Curcumin is also known to act as an immuno-modulatory molecule for SARS-CoV-2 virus and prevent viral entry and replication. Recently, curcumin showed effective binding affinity with both the viral spike [12] and host ACE2 [13] proteins to potentially inhibit the assembly of SARS-CoV-2. Turmeric-derived curcumin also exhibits potent binding affinities for the SARS-CoV-2 nucleocapsid and nsp10 proteins, comparable to those of ivermectin, azithromycin and remdesivir, thus making curcumin a potent drug to target the SARS-CoV-2 nucleocapsid protein [14].

Although generally recognized as safe (GRAS), curcumin is not widely used in a medical environment due to its low bioavailability and hydrophobic nature [14]. Utilization of the emerging class of carbon-based nanomaterials, carbon-dots, has been implemented in drug delivery systems to achieve a higher solubility and bioavailability for organic compounds [15–19]. Previous study has successfully increased the solubility and antiviral properties of curcumin by means of carbon quantum nanodots, in which curcumin-carbon quantum nanodots showed higher compatibility and antiviral activity against enterovirus 71 compared to curcumin [20].

Dimer-based screening system (DBSS) is a high-throughput screening system that utilizes synthetic biology principles to target biological systems with homodimerizing proteins. This system employs the AraC arabinose operon from *Escherichia coli* as a repressor and the emGFP fluorescent protein as a reporter [21]. Established first to target the *Mycobacterium tuberculosis* PhoR [22,23] and human immunodeficiency virus (HIV) protease [24,25] two-component systems, this system was later adapted to target the dimerization of the SARS-CoV-2 nucleocapsid [26]. Homo-dimerization of the nucleocapsid, directly facilitated by the C-terminal domain (CTD) of this protein, is integral for the nucleocapsid to form a stable conformation and properly aid viral replication [27] and should prove a fit target for the DBSS system.

In this study, we explored the effect of the construction of the curcumin-derived carbon-dots on its potential in inhibiting the dimerization of the nucleocapsid CTD (N-CTD), by means of molecular docking, dimer-based screening system (DBSS), and SARS-CoV-2-infected cell culture challenge testing.

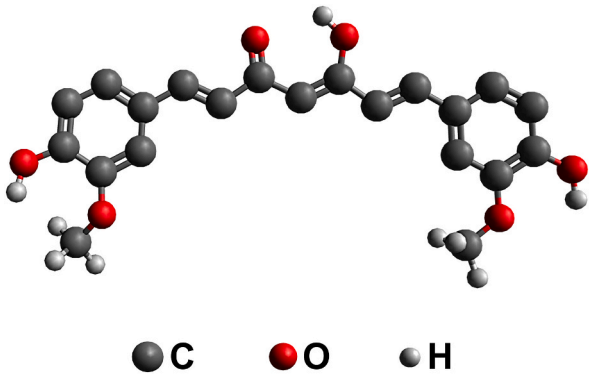

Fig. 1. Molecular structure of 1,7-bis(4-hydroxy-3-methoxyphenyl)-1,6-heptadiene-3,5-dione ($C_{21}H_{20}O_6$), or synonymously referred to as curcumin [8].

2. Materials and methods

2.1. Preliminary in-silico analysis

Molecular docking of unmodified curcumin and hypothetical structures of curcumin-derived carbon-dots (cur-CDs) on the C-terminal domain (CTD) of the SARS-CoV-2 nucleocapsid protein (PDB ID: 6ZCO) was performed using the AutoDock Vina from AutoDock Tools (1.5.6.) [28] with a 22 × 22 × 22 Å grid box at [5.264 Å, - 2.987 Å, 3.175 Å] coordinate, with a 1.00 Å spacing. Docking of drug candidates were performed on the keto and keto-enol tautomers. Docking results were visualized using the BIOVIA Discovery Studio (BIOVIA, San Diego, CA, USA). Amount of dimer residues affecting the interaction between the nucleocapsid protein and the ligand was represented as the percentage of interaction according to this calculation:

$$\%interaction = \frac{\Sigma(Dimer\ residues\ affecting\ the\ N-ligand\ interaction)}{\Sigma(Dimer\ residues\ of\ nucleocapsid\ protein)} \times 100\%$$

2.2. Preparation of curcumin and curcumin-derived carbon dots

The curcumin-derived Carbon dots (cur-CDs) was prepared through a solvothermal method. 0.3 mol of citric acid (Sigma Aldrich, USA) and 1.5 mol urea (Sigma Aldrich, USA) were stirred in deionized water at room temperature. In parallel, the 1 mmol of curcumin (Biopharma, Indonesia) was dispersed in ethanol at room temperature. Then, the curcumin dispersion was mixed with the precursors at 60 °C for 30 min. Then, the precursor was reacted in Teflon autoclave at 160 °C for 5 h. The resulted solution was filtered and purified through a centrifugation and regenerated-cellulose filter membrane 0.22 μm. Curcumin-derived CDs powder were then obtained after freezing dry. Curcumin and cur-CDs powder were dissolved in dimethyl sulfoxide (DMSO) and sterile distilled water respectively. Stock solution was protected from light and stored at −20 °C. Working solutions at 2 μg/mL, 4 μg/mL, 6 μg/mL, 8 μg/mL, and 10 μg/mL were achieved by diluting the stock in DMEM supplemented with 10% and 2% FBS for the cytotoxicity and antiviral activity assays respectively.

2.3. Screening of drug candidates using dimer-based screening system (DBSS)

Escherichia coli BL21 (DE3) containing the AraC_CTD plasmid was grown in Luria-Bertani broth (LB) supplemented with 200 ng/μL ampicillin before being subjected to a 0.4 μM IPTG induction when optical density at 600 nm (OD_{600}) reached 0.4.95 μL of culture was transferred into a 96-well LUMITRAC™ white microplate (Greiner Bio-One, Indonesia) containing 200 μg/mL ampicillin and 5 μL of drug candidate and incubated at 37 °C 200 rpm for 4 h. Fluorescence was measured in a 96-well LUMITRAC™ black microplate (Greiner Bio-One, Indonesia) at an excitation of 475 nm and emission of 500–550 nm (E535) using Glomax™ Explorer (Promega, USA) and was defined as the culture fluorescence relative to culture biomass at OD_{600} using Glomax™ Explorer (Promega, USA) [29].

2.4. Cell lines and virus

Vero E6 cells were maintained in Dulbecco's Modified Eagle's Medium (DMEM; Sigma-Aldrich, USA) supplemented with 10% fetal bovine serum (FBS; Gibco, USA), and 1% penicillin/streptomycin (Sigma-Aldrich, USA). Cells were maintained at 37 °C in a 5% CO_2 humidified (95%–99% humidity) incubator. Infections were performed using propagations of the B.1.459 strain of the SARS-CoV-2 swab specimen, isolated from Bogor, Indonesia in May 2020 (EPI_ISL_4004658).

2.5. Cytotoxicity assay

200 μl of Vero E6 cells in DMEM supplemented with 10% FBS at a density of 2×10^4 cells/well were seeded into 96-well plates and incubated for 24 h at 37 °C in 5% CO_2. After reaching >80% confluence, observed under inverted microscope (Leica Microsystems), supernatant was removed, followed by the addition of 100 μL of DMEM supplemented with 10% FBS containing curcumin and cur-CDs at a final concentration of 4 μg/mL, 6 μg/mL, 8 μg/mL, and 10 μg/mL into the plate in triplicates for an incubation period of 72 h. Afterwards, supernatant was removed, cells were washed with phosphate buffered saline (PBS), and 100 μL of 3-(4,5-dimethylthiazol-2-yl)-2,5-diphenyltetrazolium bromide (MTT) at 0.5 mg/mL was added. The plates were incubated for 4 h at 37 °C in 5% CO_2, protected from light, and 100 μL DMSO was used to stop mitochondrial activity. Plates were gently rocked on a platform rocker for 10 min to allow the formazan product to solubilize. Intensity of the formazan product was measured at 570 nm using the Multiskan™ GO Microplate Spectrophotometer (ThermoScientific, USA). The average absorbance of the DMEM media was used as blank and the average absorbance of untreated cells was used as negative control. Cell viability of treated wells was expressed as the percentage of the negative control. Concentrations where cells reached a viability of 70% or more were considered non-cytotoxic. 50% cytotoxicity concentration (CC_{50}) values of curcumin and curcumin-nanodots were acquired by means of linear regression.

2.6. Antiviral activity assay

Vero E6 cells in DMEM supplemented with 10% FBS at a density of 2×10^4 cells/well were seeded into 96-well plates and incubated for 24 h at 37 °C in 5% CO_2. After reaching >80% confluence, observed under inverted microscope (Leica Microsystems), supernatant

was removed, plates were transferred to a BSL-3 facility, and supernatant was removed. SARS-CoV-2 culture in DMEM supplemented with 2% FBS (MOI = 0.1) were inoculated into the plates. Plates were incubated at 37 °C 1 h, with shaking at 15-min intervals to ensure maximum viral adsorption. Removal of supernatant was followed by the addition of 100 μL of DMEM supplemented with 2% FBS containing curcumin and cur-CDs at a final concentration of 4 μg/mL, 6 μg/mL, 8 μg/mL, and 10 μg/mL into the plate in twelve replicates. Plates were incubated for 72 h at 37 °C, and cytopathic effects on Vero E6 cells were observed using the ZOE Fluorescent Cell Imager (Bio-Rad). Wells displaying signs of cell death were considered affected by cytopathic effects. Plates were then fixated using 4% formaldehyde, and stained using 0.5% crystal violet solution.

Further investigation on the maximum virus titer susceptible to curcumin and cur-CDs were performed by selecting the lowest drug candidate concentration where no cytopathic effect was observed in the previous experiment. Antiviral activity assay was performed to challenge drug candidates at virus concentrations in serial increase.

2.7. Statistical analyses

All data processing and statistical analysis was performed using Microsoft Excel (Microsoft, USA) and SPSS Statistics (IBM, USA), with values expressed as mean ± standard deviation (SD). Statistical analysis was performed using Student's t-test for parametric data or Chi-square test for non-parametric data, where $p \leq 0.05$ was considered significantly different. For the DBSS, homogeneity and significance of normalized fluorescence values were analyzed using Levene's test and one-way ANOVA, followed by post-hoc analysis using Tukey's test, where $p \leq 0.05$ was considered significantly different.

3. Results

3.1. Preliminary in-silico analyses

To investigate the binding affinity and %interaction between SARS-CoV-2 N-CTD (PDB ID: 6ZCO) with drug candidates, we performed *in-silico* molecular docking predictions on curcumin and several hypothetical curcumin-derived carbon-dots (cur-CDs) structures (amino, graphitic, pyridinic, and pyrrolic) in their respective keto and keto-enol tautomers, available in Supplementary Materials Fig. S1.

As shown in Fig. 2a, all candidates resulted in negative free energy values for binding affinity, indicating spontaneous interactions between drug candidates and N-CTD. Fig. 2b also showed all hypothetical structures of curcumin-derived carbon-dots (cur-CDs) resulting in significantly higher affinity and %interaction with N-CTD ($p \leq 0.05$) than curcumin in both its keto and keto-enol tautomers.

Quick three- and two-dimensional visualization of the molecular interaction and docking of curcumin and cur-CDs (represented by curcumin-pyridinic) were shown below in Fig. 3. Curcumin interacted with fourteen residues of N-CTD, seven of which are non-bonding van der Waals forces, as shown in Fig. 3a, with three-dimensional visualizations of these interactions shown in Fig. 3c. Modification into carbon-dots nanostructure shifted the nature of the interactions into more non-covalent bonding pi bond interactions, all of which interact with cur-CDs in more than one site of the molecule, shown in Fig. 3b and d. A visible increase of bonding interactions, from eleven interactions facilitated by seven residues to twenty interactions facilitated by seven residues, can be observed when modifying curcumin to its carbon-dots structure. Almost all the residues participating in the binding of curcumin and cur-CDs with the N-CTD are residues that facilitate the dimerization of N-CTD. These residues interacted strongly via hydrogen

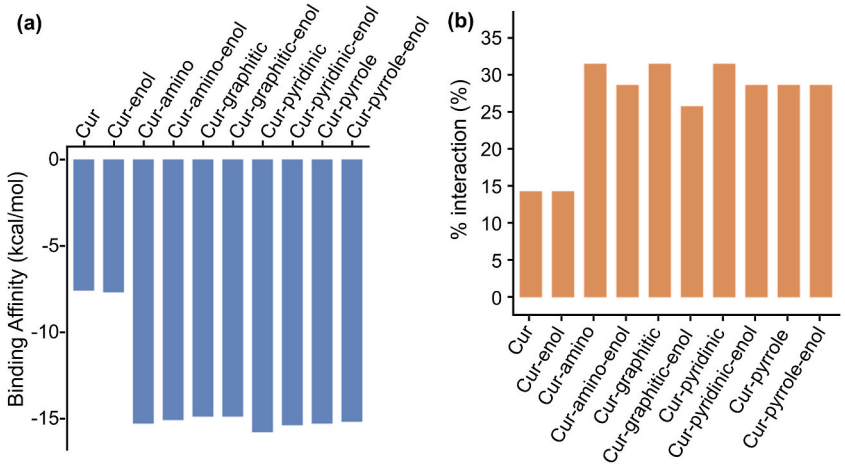

Fig. 2. (A) Binding affinity (kcal/mol) and (b) %interaction between SARS-CoV-2 N-CTD with curcumin and cur-CDs in both its keto and keto-enol tautomers. Curcumin and cur-CDs all resulted in spontaneous binding, and all hypothetical structures of cur-CDs resulted in more spontaneous binding and higher %interaction.

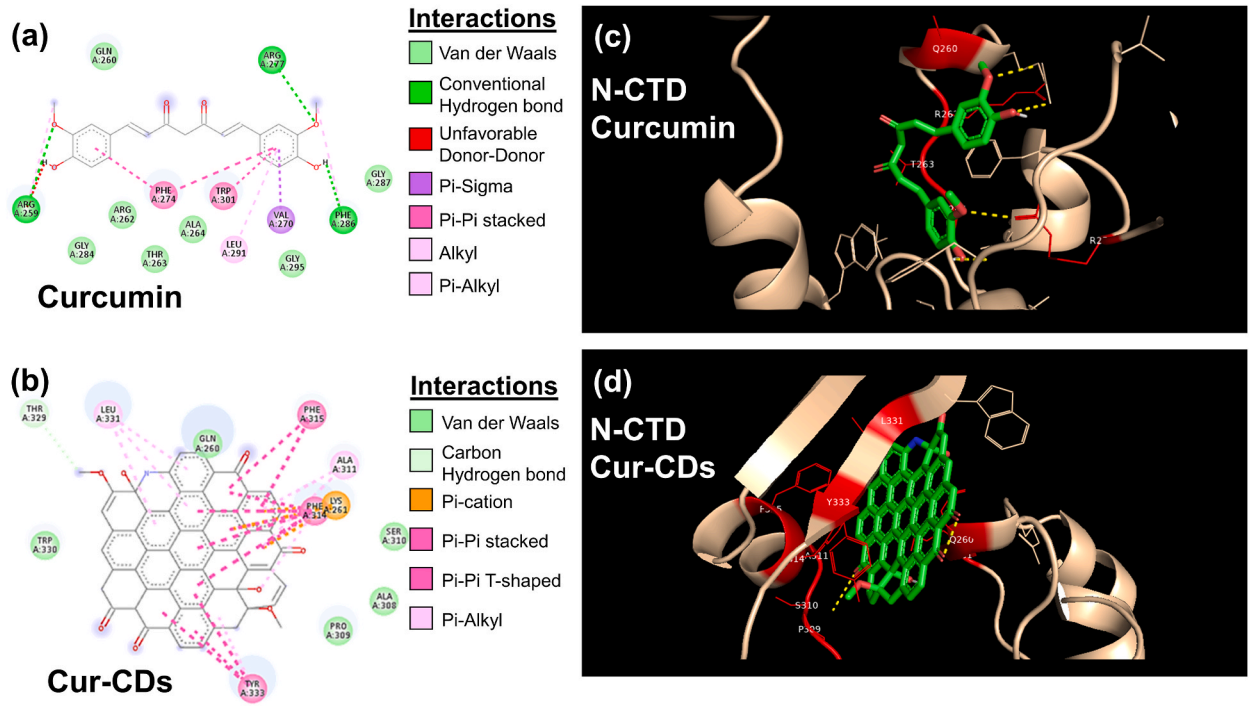

Fig. 3. Two-dimensional visualization of the interaction between the N-CTD and (a) curcumin and (b) cur-CDs, and three-dimensional visualization of the interaction between the N-CTD with (c) curcumin and (d) cur-CDs. Modification of curcumin into cur-CDs resulted in more bonding interactions between cur-CDs and SARS-CoV-2 N-CTD.

bonding in the dimerization of the N-CTD [30], but only interacted weakly via van der Waals forces and non-covalent interactions in curcumin and cur-CDs.

3.2. *Screening of drug candidates using the dimer-based screening system (DBSS)*

The dimerization inhibition activity of the drug candidates was then proved using the dimer-based screening system (DBSS) that targets the dimerization of the SARS-CoV-2 nucleocapsid. Using this screening system, treatment with curcumin at 4–8 μg/mL significantly inhibited the dimerization of nucleocapsid compared to a baseline of 0 μg/mL treatment ($p \leq 0.05$), indicated by higher fluorescence values, and functioned most effectively at 6 and 8 μg/mL, as shown below in Fig. 4a. A visible change in trend could be observed in treatment of cur-CDs, in Fig. 4b, where increase of drug concentration gave steeper increase of corrected fluorescence. Cur-CDs were effective at 4–10 μg/mL, peaking at 8–10 μg/mL where fluorescence reached 3417.2 ± 338.36 and 3251.5 ± 304.14.

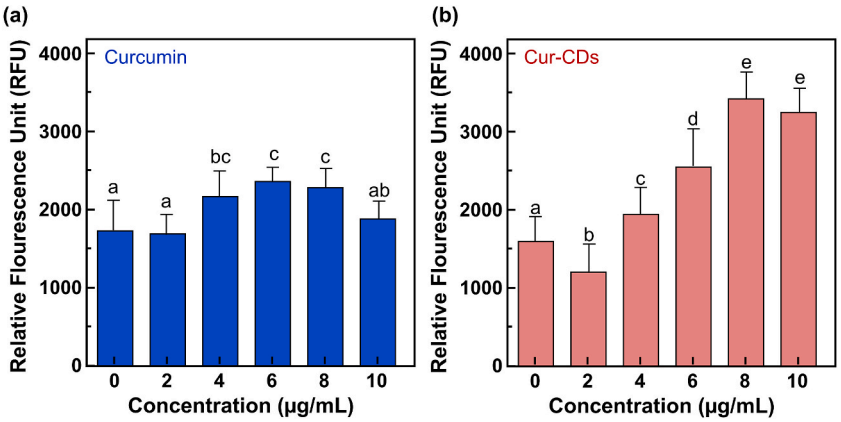

Fig. 4. Inhibition of nucleocapsid dimerization by (a) curcumin and (b) cur-CDs observed in the dimer-based screening system (n = 10). Increase of curcumin and cur-CDs concentration significantly enhance the effectiveness of curcumin and cur-CDs in inhibiting N-CTD dimerization, except for curcumin 2 μg/mL. Different lower-case letters represent significantly different means according to Tukey's post-hoc test ($p \leq 0.05$).

Treatment of curcumin and cur-CDs at 2 μg/mL did not result in a significantly higher fluorescence, showing their incapability to inhibit the dimerization of the viral protein, and was eliminated from further investigation.

3.3. Dose-dependent cytotoxicity and antiviral activity of curcumin and cur-CDs on Vero E6 cells

Cytotoxicity assay on Vero E6 cells was performed to investigate the cytotoxicity of curcumin and cur-CDs on mammalian cells. Measurement of drug candidates at 0 μg/mL was represented by viability in respective solvents. Use of DMSO 1% did not result in lower viability compared to untreated cells, as have previously been reported [31].

Treatment of curcumin and cur-CDs resulted in a negatively-sloped trend and were all within a non-toxic range, shown in red in Fig. 5a and b respectively. Treatment of curcumin and cur-CDs at 4–10 μg/mL both did not give strong correlation with Vero E6 viability by means of regression R^2. Using linear regression, curcumin and cur-CDs were found to reach CC_{50} at 30 μg/mL and 11.67 μg/mL. A higher CC_{50} value from treatment of curcumin might be indicative of curcumin imparting a beneficial effect on cell growth.

Primary investigation for the antiviral activity of curcumin and cur-CDs against N-CTD were performed by separately culturing Vero E6 cells with treatment of curcumin and cur-CDs at different concentrations for 72 h after infection of SARS-CoV-2 at MOI = 0.1. Results are all shown below in Fig. 5, with visual and microscopic observations available in Supplementary Materials Tables S2 and S3.

Shown in blue in Fig. 5a and b, increasing the concentration of curcumin increased cell viability to 83.3%, peaking at 6 μg/mL where %CPE reached 0%. However, when modified into carbon-dots structure, post-infection treatment of as little as 4 μg/mL of cur-CDs effectively stopped any cytopathic effect from SARS-CoV-2, indicating the heightened effectiveness of the carbon-dots structure in inhibiting the N-CTD dimerization.

Further investigation of the maximum SARS-CoV-2 virus titer was performed with cur-CDs at 4 μg/mL, with results shown in Table 1. SARS-CoV-2 at MOI = 1.6 resulted in 100% CPE for control and cur-CDs, thus investigation at higher virus titers were not performed. Presence of cur-CDs resulted in increased %viability, reaching a maximum just before MOI = 0.8.

4. Discussion

Our study aims to explore the modification of curcumin into its carbon-dots structure as a potential COVID-19 antiviral drug. Curcumin has been documented exhibiting antiviral properties against SARS-CoV-2 by means of immune modulation, prevention of viral attachment [12,13], and recently by binding to nucleocapsid in a manner comparable to ivermectin, azithromycin and remdesivir [14].

Significant increases in both binding affinity and %interaction observed when comparing curcumin and hypothetical curcumin-derived carbon-dots structures are strong indications of effectiveness of carbon-dots structures in interacting with the N-CTD. With binding affinity levels ranging from −14.9 kcal/mol to −15.8 kcal/mol, cur-CDs show more potential in binding with SARS-CoV-2 N-CTD than several approved, clinical trials, and pre-clinical trials nucleocapsid-targeting drugs [32], including: rapamycin (ΔG = −8.91 kcal/mol), silmitasertib (ΔG = −7.89 kcal/mol), TMCB (ΔG = −7.05 kcal/mol), and sapanisertib (ΔG = −6.14 kcal/mol) [27]. For comparison, other antiviral drugs, including lopinavir (ΔG = −6.58 kcal/mol), remdesivir (ΔG = −3.46 kcal/mol), chloroquine (ΔG = −5.62 kcal/mol), favipiravir (ΔG = −4.44 kcal/mol), ribavirin (ΔG = −4.86 kcal/mol), hydroxychloroquine (ΔG = −4.32 kcal/mol), and oseltamivir (ΔG = −5,08 kcal/mol) showed weaker binding affinity when docked to the SARS-CoV-2 nucleocapsid dimerization domain (PDB ID: 6WZQ) [33].

Modification of precursor curcumin into a carbon-dots structure also offers a solution to the low bioavailability and hydrophobic nature of curcumin. Indeed, when comparing the aqueous solubility of curcumin and curcumin-derived carbon quantum dots, Lin et al.

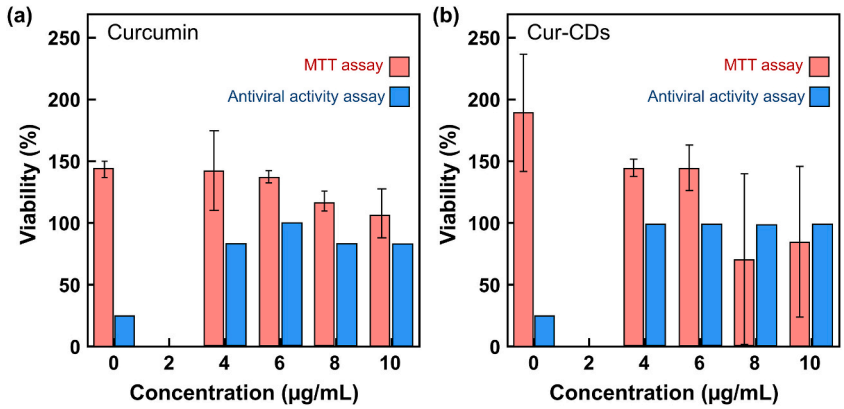

Fig. 5. Vero E6 cells viability treated with (a) curcumin, and (b) cur-CDs after 72 h. Viability from MTT assay is expressed as mean percentage ± standard deviation compared to treatment of solvents (n = 3) and viability from antiviral activity assay is expressed as %no-CPE (n = 6). Cur-CDs showed a steeper trend in viability decrease in the MTT assay compared to curcumin but resulted in 100% viability (0% CPE) with treatment as little as 4 μg/mL. Curcumin resulted in 83.3% viability and peaked at 6 μg/mL, where %CPE reached 0%.

Table 1
%CPE reduction values of cur-CDs. %viability is expressed as %no-CPE (n = 12). Cur-CDs at 4 μg/mL effectively increased the viability of Vero-E6 cells until reaching a maximum SARS-CoV-2 titer at MOI = 0.8.

Drug candidate	MOI	%viability vehicle	%viability drug	%viability increase
cur-CDs	1.6	0	0	0%
4 μg/mL	0.8	0	0	0%
	0.4	0	8.3	8.3%
	0.2	33.3	41.6	8.3%
	0.1	50	91.7	41.7%

observed a significant difference between 3.12 μg/mL and >50 mg/mL [20], and Chen et al. observed a similarly significant difference between $<10^{-2}$ mg/mL and 50 mg/mL [17].

Confirming the *in-silico* results, the dimerization inhibition activity of curcumin and cur-CDs were further explored using the dimer-based screening system (DBSS). In the earlier studies, DBSS adopts the two-component system (TCS) in bacteria, consisting of histidine kinase (HK) and response regulators (RR) [34,35]. DBSS utilizes the ability of cytoplasmic HKs to dimerize *in vitro*, and a promoter-repressor pair to receive a signal from HKs [23,34–36]. Designed as a tool for preliminary drug screening, the DBSS system, previously employing the *M. tuberculosis* PhoR and HIV-1 protease dimers, has been used in the discovery of black caraway (*Nigella sativa*) compounds JH-1 and JH-3 as antitubercular and antiretroviral drugs [21–24,37–39]. A new system, now employing the fusion of N-CTD as a dimer-binding domain and the araC promoter/repressor system as a DNA-binding domain, has been designed to target the dimerization of SARS-CoV-2 N-CTD and allow the detection and quantification of the N-CTD dimerization in the presence of candidate drugs [26,40].

Heightened inhibition of N-CTD was confirmed in the DBSS system, where cur-CDs resulted in a significant increase of fluorescence across all concentrations ($p < 0.05$).

Primary investigation into the antiviral activity of curcumin and cur-CDs was performed using the B.1.459 strain of the SARS-CoV-2 (EPI_ISL_4004658). To account for the differences in the N-CTD structures between this strain and other variants of SARS-CoV-2, we performed comparison between the nucleocapsid sequences of different SARS-CoV-2 lineages and variants and found no synonymous mutations between the N-CTD of the B.1.459 strain of the SARS-CoV-2 and that of the Alpha, Beta, Gamma, Delta, Omicron, XBB.1, XBB.1.5.X, and Omicron BA.2.75.X [41]. A similar previous inquiry also showed curcumin exhibiting antiviral activity in a manner independent of SARS-CoV-2 strains and variants [5].

Treatment of curcumin has been documented reducing the viability of other cell lines, where treatment of 10 μg/mL curcumin resulted in less than 10% of fibroblasts BHK-21 cells viability [17]. Kumbar et al. and Lin et al. documented half-maximal cytotoxicity concentrations of curcumin at 8.84 and 13 μg/mL using the oral cancer (KB) and rhabdomyosarcoma (RD) cell line [20,42]. However, we observed treatment of up to 10 μg/mL of curcumin to be non-toxic, with a CC_{50} value at 30 μg/mL. Plant extracts with CC_{50} values higher than 20 μg/mL are considered non- or weakly cytotoxic on the mammalian cells [43]. This is closer to the observation made by Marín-Palma et al., where treatment of curcumin on Vero E6 cells resulted in cytotoxicity after 48 h at concentrations higher than 10 μg/mL [5], and by Khosropanah et al. where curcumin reached half-maximal cytotoxicity concentrations at 30.78 μg/mL for epithelial human breast cancer MDA-MB-231 cell line after 72 h [44].

In contrast, treatment of our cur-CDs resulted in a lower CC_{50} value, almost by a third. This may be attributed to the fluctuating reading of cur-CDs viability or the incompatibility with the cell line that we used. Indeed after 24 h of incubation on human rhabdomyosarcoma cells, other carbon-dots derivatives of curcumin can be observed reaching CC_{50} values 3.8 (50.0 μg/mL) to ≈35-fold (452.2 μg/mL) higher than curcumin [20]. 24 h of incubation on BHK-21 cells even resulted in curcumin carbon-dots reaching a CC_{50} value 50-fold higher than curcumin [17]. As a comparison, COVID-19 drugs remdesivir and ritonavir has a CC_{50} value of >100 μM (≈62.0 μg/mL) and 94.71 μmol/L (≈68.3 μg/mL) on Vero E6 cells, respectively [45–47].

Post-infection treatment of curcumin resulted in increased cell viability to 83.3%, suggesting antiviral activity, with 0% cytopathic effect observed at 6 μg/mL. At a lower SARS-CoV-2 titer (MOI = 0.01), quantified observation of antiviral activity of curcumin at 1.25 μg/mL to 10 μg/mL showed a similar result with 87% inhibition [5].

However, cur-CDs exhibited more potent protection, with 100% cell viability with as little as 4 μg/mL treatment, signifying a significant increase of effectiveness in modification of curcumin into its carbon-dots structure. At 4 μg/mL, cur-CDs exerted antiviral activity up to just before SARS-CoV-2 titer reached MOI = 0.8. As a comparison, COVID-19 drug remdesivir reached half-maximal inhibitory concentration at 9.2 μM (≈5.5 μg/mL) on Vero E6 cells infected with SARS-CoV-2 at MOI = 0.1 [46,48] and ritonavir at 19.88 μM (≈14.3 μg/mL) on Vero E6 cells infected with WIV04 SARS-CoV-2 at MOI = 0.2 [47,49]. Baricitinib, a JAK1/JAK2 inhibitor approved for COVID-19 treatment, reached half-effective concentration at 5.9 μM (≈2.191 μg/mL) and 5.7 μM (≈2.117 μg/mL) for JAK1 and JAK2 respectively [50,51].

Indeed, modification of curcumin into curcumin-derived carbon quantum dots have also been observed resulting in significant decrease of enterovirus 71 plaque-forming units [20]. In addition to improved solubility and increased bioavailability, heightened antiviral activity in cur-CDs can also be explained by its carbon-dots nanostructures, which may display higher densities of curcumin moieties to interact with SARS-CoV-2 [20]. Curcumin-derived carbon quantum dots synthesized by Lin et al. were observed to contain a high density of curcumin-relative polymers on the carbon-dots surface, enabling the compound to act against the enterovirus 71 in various stages of the virus cycle through different mechanisms. Possible structural changes and degradation of curcumin molecules during the synthesis of curcumin-derived carbon quantum dots could also explain the reduced cytotoxic properties of curcumin and

boosted its antiviral activity [20].

Additionally, the higher effectivity in the inhibition of SARS-CoV-2 N-CTD dimerization displayed by cur-CDs in the DBSS has been successfully confirmed by the heightened antiviral activity of cur-CDs *in vitro*. This may suggest high-throughput screening systems such as the Dimer-Based Screening System design as a practical solution to study molecular mechanisms of pathogenic agents in a safer environment and lower biosafety risks.

5. Limitations and future research

An interesting feature to explore would be the effect of pre-infection treatment of curcumin and cur-CDs against SARS-CoV-2 to gain a more comprehensive insight into the complete mode-of-action of the antiviral candidates. Curcumin was observed inhibiting the infection of SARS-CoV-2 D614G strain by a proposed mechanism of prevention of host cell recognition and entry by directly interacting with host or viral proteins. In addition to the early stages of SARS-CoV-2 infection, pre-infection treatment of curcumin can also shed light into the immuno-modulatory properties of curcumin. Curcumin is known to prevent the onset of the cytokine storm, which plays a central role in COVID-19 symptoms [5]. Pre-infection treatment of cur-CDs should help illuminate the advantage of carbon-dots structures in amplifying the antiviral activity of curcumin to inhibit SARS-CoV-2 infection.

Cytotoxicity assays of curcumin and cur-CDs on other cell lines can provide valuable insights into the cytotoxic nature of cur and cur-CDs in different cells. Furthermore, treatment of curcumin and cur-CDs in vivo should give insights into the comprehensive mechanism of curcumin and its carbon-dots derivatives in combating SARS-CoV-2 infection. Moreover, cellular uptake and solubility assays become imperative in establishing the bioavailability of curcumin and cur-CDs.

By employing a similar approach, future research on the antiviral activity of natural compounds can be accomplished by modifying natural compounds into their carbon-dots derivatives to improve their bioactivities. Additionally, by substituting the use of viable viruses with *E. coli*, the DBSS can serve as a preliminary screening system before conducting the experiment properly in a higher biosafety level laboratory.

6. Conclusions

To the best of our knowledge, our study is the first to propose the utilization of curcumin-derived carbon-dots (cur-CDs) to fight SARS-CoV-2 infection. Modification of curcumin into cur-CDs resulted in significantly higher affinity and %interaction with N-CTD. DBSS results also showed cur-CDs exhibiting higher antiviral activity compared to curcumin. We observed CC_{50} values of curcumin and cur-CDs at 30 μg/mL and 11.67 μg/mL on Vero E6 cells. Post-infection treatment of 6 μg/mL curcumin and 4 μg/mL cur-CDs resulted in 0% CPE in SARS-CoV-2-infected Vero E6 cells. Thus, this study demonstrated the higher effectiveness of cur-CDs, in comparison to curcumin, in inhibiting the dimerization of SARS-CoV-2 N-CTD as well as disrupting the infection of the coronavirus to its host cells.

Author contribution statement

Azzania Fibriani; Ernawati Arifin Giri-Rachman: Conceived and designed the experiments; Contributed reagents, materials, analysis tools or data; Wrote the paper.

Audrey Angelina Putri Taharuddin: Conceived and designed the experiments; Performed the experiments; Analyzed and interpreted the data; Wrote the paper.

Rebecca Stephanie; Nicholas Yamahoki: Performed the experiments; Analyzed and interpreted the data; Wrote the paper.

Jessica Laurelia; Yana Rubiyana: Performed the experiments; Analyzed and interpreted the data.

Popi Hadi Wisnuwardhani; Dian Fitria Agustiyanti; Marissa Angelina: Contributed materials and designed experiments; Performed the experiments; Analyzed and interpreted the data.

Ratih Asmana Ningrum; Andri Wardiana; Ferry Iskandar; Fitri Aulia Permatasari: Contributed reagents, materials, analysis tools or data.

Data availability statement

Data included in article/supplementary material/referenced in article.

Declaration of competing interest

The authors declare that they have no known competing financial interests or personal relationships that could have appeared to influence the work reported in this paper.

Acknowledgementss

We would like to acknowledge Muhammad Hamzah Syaifullah Azmi and Vergio Victorio Effendy for the establishment of the novel nucleocapsid-targeting dimer-based screening system used in this study. This research was funded by the Indonesian National Research and Innovation Agency (BRIN) [grant number 60/II/HK/2022]; Bandung Institute of Technology [grant number SITH.PPMI-1-50-2021]; and the Indonesian Endowment Fund for Education and the Indonesian Science Fund through the International

Collaboration RISPRO Funding Program [grant number RISPRO/KI/B1/KOM/11/4542/2/2020].

Appendix A. Supplementary data

Supplementary data to this article can be found online at https://doi.org/10.1016/j.heliyon.2023.e20089.

References

[1] World Health Organization, WHO Coronavirus (COVID-19) Dashboard, 2023. https://covid19.who.int/. (Accessed 26 January 2023).

[2] M. Kumari, R.M. Lu, M.C. Li, J.L. Huang, F.F. Hsu, S.H. Ko, F.Y. Ke, S.C. Su, K.H. Liang, J.P.Y. Yuan, H.L. Chiang, C.P. Sun, I.J. Lee, W.S. Li, H.P. Hsieh, M.H. Tao, H.C. Wu, A critical overview of current progress for COVID-19: development of vaccines, antiviral drugs, and therapeutic antibodies, J. Biomed. Sci. 291 (2022) 1–36, https://doi.org/10.1186/S12929-022-00852-9, 2022, 29.

[3] J. Zahradník, S. Marciano, M. Shemesh, E. Zoler, D. Harari, J. Chiaravalli, B. Meyer, Y. Rudich, C. Li, I. Marton, O. Dym, N. Elad, M.G. Lewis, H. Andersen, M. Gagne, R.A. Seder, D.C. Douek, G. Schreiber, SARS-CoV-2 variant prediction and antiviral drug design are enabled by RBD in vitro evolution, Nat. Microbiol. 69 (6) (2021) 1188–1198, https://doi.org/10.1038/s41564-021-00954-4, 2021.

[4] U.S. Food and Drug Administration, Coronavirus (COVID-19) | Drugs, 2023. https://www.fda.gov/drugs/emergency-preparedness-drugs/coronavirus-covid-19-drugs. (Accessed 11 July 2023).

[5] D. Marín-Palma, J.H. Tabares-Guevara, M.I. Zapata-Cardona, L. Flórez-álvarez, L.M. Yepes, M.T. Rugeles, W. Zapata-Builes, J.C. Hernandez, N.A. Taborda, Curcumin inhibits in vitro SARS-CoV-2 infection in Vero E6 cells through multiple antiviral mechanisms, Mol 26 (2021) 6900, https://doi.org/10.3390/MOLECULES26226900, 2021, 26, 6900.

[6] Z. Bai, Y. Cao, W. Liu, J. Li, The SARS-CoV-2 nucleocapsid protein and its role in viral structure, biological functions, and a potential target for drug or vaccine mitigation, Viruses 13 (2021) 1115, https://doi.org/10.3390/V13061115, 2021, 13, 1115.

[7] N.K. Dutta, K. Mazumdar, J.T. Gordy, The nucleocapsid protein of SARS–CoV-2: a target for vaccine development, J. Virol. 94 (2020), https://doi.org/10.1128/JVI.00647-20.

[8] J. Sharifi-Rad, Y. El Rayess, A.A. Rizk, C. Sadaka, R. Zgheib, W. Zam, S. Sestito, S. Rapposelli, K. Neffe-Skocińska, D. Zielińska, B. Salehi, W.N. Setzer, N. S. Dosoky, Y. Taheri, M. El Beyrouthy, M. Martorell, E.A. Ostrander, H.A.R. Suleria, W.C. Cho, A. Maroyi, N. Martins, Turmeric and its major compound curcumin on health: bioactive effects and safety profiles for Food, pharmaceutical, biotechnological and medicinal applications, Front. Pharmacol. 11 (2020) 1021, https://doi.org/10.3389/FPHAR.2020.01021/BIBTEX.

[9] J.R. de Oliveira, B.S. Antunes, G.O. do Nascimento, J.C. de S. Kawall, J.V.B. Oliveira, K.G. dos S. Silva, M.A. de T. Costa, C.R. Oliveira, Antiviral activity of medicinal plant-derived products against SARS-CoV-2, Exp. Biol. Med. 247 (2022) 1797, https://doi.org/10.1177/15353702221108915.

[10] M. Butnariu, C. Quispe, N. Koirala, S. Khadka, C.M. Salgado-Castillo, M. Akram, R. Anum, B. Yeskaliyeva, N. Cruz-Martins, M.M.M. Kumar, R.V. Bagiu, A.F. A. Razis, U. Sunusi, R.M. Kamal, J. Sharifi-Rad, Bioactive effects of curcumin in human immunodeficiency virus infection along with the most effective isolation techniques and type of nanoformulations, Int. J. Nanomed. 17 (2022) 3619, https://doi.org/10.2147/IJN.S364501.

[11] E.A. Sianipar, The potential of Indonesian traditional herbal medicine as immunomodulatory agents: a review, Int. J. Pharm. Sci. Res. (2021). https://ijpsr.com/bft-article/the-potential-of-indonesian-traditional-herbal-medicine-as-immunomodulatory-agents-a-review/. (Accessed 26 January 2023).

[12] A.B. Jena, N. Kanungo, V. Nayak, G.B.N. Chainy, J. Dandapat, Catechin and curcumin interact with S protein of SARS-CoV2 and ACE2 of human cell membrane: insights from computational studies, 2021 111, Sci. Rep. 11 (2021) 1–14, https://doi.org/10.1038/s41598-021-81462-7.

[13] H. Noor, A. Ikram, T. Rathinavel, S. Kumarasamy, M. Nasir Iqbal, Z. Bashir, Immunomodulatory and anti-cytokine therapeutic potential of curcumin and its derivatives for treating COVID-19 – a computational modeling 40 (2021) 5769–5784, https://doi.org/10.1080/07391102.2021.1873190.

[14] R. Suravajhala, A. Parashar, G. Choudhir, A. Kumar, B. Malik, V.A. Nagaraj, G. Padmanaban, R. Polavarapu, P. Suravajhala, P.B.K. Kishor, Molecular docking and dynamics studies of curcumin with COVID-19 proteins, Netw. Model. Anal. Heal. Informatics Bioinforma. 10 (2021), https://doi.org/10.1007/S13721-021-00312-8.

[15] S. Kotta, H.M. Aldawsari, S.M. Badr-Eldin, N.A. Alhakamy, S. Md, A.B. Nair, P.K. Deb, Exploring the potential of carbon dots to combat COVID-19, Front. Mol. Biosci. 7 (2020) 428, https://doi.org/10.3389/FMOLB.2020.616575/BIBTEX.

[16] A. Shafi, S. Bano, S. Sabir, M.Z. Khan, M.M. Rahman, A. Shafi, S. Bano, S. Sabir, M.Z. Khan, M.M. Rahman, Eco-friendly fluorescent carbon nanodots: characteristics and potential applications, Carbon-Based Mater. Environ. Prot. Remediat. (2020), https://doi.org/10.5772/INTECHOPEN.89474.

[17] H.H. Chen, C.J. Lin, A. Anand, H.J. Lin, H.Y. Lin, J.Y. Mao, P.H. Wang, Y.J. Tseng, W.S. Tzou, C.C. Huang, R.Y.L. Wang, Development of antiviral carbon quantum dots that target the Japanese encephalitis virus envelope protein, J. Biol. Chem. 298 (2022), https://doi.org/10.1016/J.JBC.2022.101957, 101957–101957.

[18] A. Kalkal, P. Allawadhi, R. Pradhan, A. Khurana, K.K. Bharani, G. Packirisamy, Allium sativum derived carbon dots as a potential theranostic agent to combat the COVID-19 crisis, Sensors Int 2 (2021), 100102, https://doi.org/10.1016/J.SINTL.2021.100102.

[19] T. Tong, H. Hu, J. Zhou, S. Deng, X. Zhang, W. Tang, L. Fang, S. Xiao, J. Liang, Glycyrrhizic-acid-based carbon dots with high antiviral activity by multisite inhibition mechanisms, Small 16 (2020), https://doi.org/10.1002/SMLL.201906206.

[20] C.J. Lin, L. Chang, H.W. Chu, H.J. Lin, P.C. Chang, R.Y.L. Wang, B. Unnikrishnan, J.Y. Mao, S.Y. Chen, C.C. Huang, High amplification of the antiviral activity of curcumin through transformation into carbon quantum dots, Small 15 (2019), 1902641, https://doi.org/10.1002/SMLL.201902641.

[21] I.D.A.P. Dwipayana, Y.M. Syah, R. Aditama, Feraliana, A. Fibriani, Development of a dimer-based screening system for dimerization inhibitor of HIV-1 protease, J. Microb. Syst. Biotechnol. 2 (2020) 1–11, https://doi.org/10.37604/JMSB.V2I2.42.

[22] E.A. Giri-Rachman, N. Steven, M. Rahmita, A. Fibriani, Produk Bakteri Escherichia Coli Yang Dimodifikasi Secara Genetik Untuk Penapisan Cepat Kandidat Obat Antituberkulosis Baru, P00201704939, 2019. https://pdki-indonesia.dgip.go.id/detail/P00201704939?type=patent&keyword=P00201704939.

[23] N. Steven, Pengembangan Dan Pengujian Sistem Penapisan Senyawa Organik Penghambat Pembentukan Dimer Domain Sitoplasmik PhoR Mycobacterium tuberculosis, Bandung Institute of Technology, School of Life Sciences and Technology, 2017.

[24] A. Fibriani, E.A. Giri-Rachman, Feraliana, N. Steven, Produk Bakteri Escherichia coli Yang Dimodifikasi Secara Genetik Untuk Penapisan Cepat Kandidat Obat HIV (Human Immunodeficiency Virus) Baru, 2018, P00201810374. https://pdki-indonesia.dgip.go.id/detail/P00201810374?type=patent&keyword=P00201810374.

[25] A. Fibriani, E.A. Giri-Rachman, Feraliana, N. Steven, I.D.A.P. Dwipayana, Metode Seleksi Kandidat Senyawa Penghambat Pembentukan Dimer Protease HIV-1, P00201810375, 2018. https://pdki-indonesia.dgip.go.id/detail/P00201810375?type=patent&keyword=P00201810375.

[26] A. Fibriani, Giri, E.A. Rachman, A.A.P. Taharuddin, M.H.S. Azmi, Plasmid rekombinan untuk penapisan cepat kandidat obat anti-sars-cov-2 yang menarget protein nukleokapsid, N) SARS-COV-2, P00202109660, 2021.

[27] S. Ahamad, D. Gupta, V. Kumar, Targeting SARS-CoV-2 nucleocapsid oligomerization: insights from molecular docking and molecular dynamics simulations, J. Biomol. Struct. Dyn. 40 (2022) 2430–2443, https://doi.org/10.1080/07391102.2020.1839563.

[28] O. Trott, A.J. Olson, AutoDock Vina: improving the speed and accuracy of docking with a new scoring function, efficient optimization, and multithreading, J. Comput. Chem. 31 (2010) 455–461, https://doi.org/10.1002/JCC.21334.

[29] L. Stiner, L.J. Halverson, Development and characterization of a green fluorescent protein-based bacterial biosensor for bioavailable toluene and related compounds, Appl. Environ. Microbiol. 68 (2002) 1962, https://doi.org/10.1128/AEM.68.4.1962-1971.2002.

[30] R. Zhou, R. Zeng, A. von Brunn, J. Lei, Structural characterization of the C-terminal domain of SARS-CoV-2 nucleocapsid protein, Mol. Biomed. 1 (2020), https://doi.org/10.1186/S43556-020-00001-4.
[31] Q. Li, C. Maddox, L. Rasmussen, J.V. Hobrath, L.E. White, Assay development and high-throughput antiviral drug screening against Bluetongue virus, Antivir. Res. 83 (2009) 267, https://doi.org/10.1016/J.ANTIVIRAL.2009.06.004.
[32] D.E. Gordon, G.M. Jang, M. Bouhaddou, J. Xu, K. Obernier, K.M. White, M.J. O'Meara, V. V Rezelj, J.Z. Guo, D.L. Swaney, T.A. Tummino, R. Hüttenhain, R. M. Kaake, A.L. Richards, B. Tutuncuoglu, H. Foussard, J. Batra, K. Haas, M. Modak, M. Kim, P. Haas, B.J. Polacco, H. Braberg, J.M. Fabius, M. Eckhardt, M. Soucheray, M.J. Bennett, M. Cakir, M.J. McGregor, Q. Li, B. Meyer, F. Roesch, T. Vallet, A. Mac Kain, L. Miorin, E. Moreno, Z.Z.C. Naing, Y. Zhou, S. Peng, Y. Shi, Z. Zhang, W. Shen, I.T. Kirby, J.E. Melnyk, J.S. Chorba, K. Lou, S.A. Dai, I. Barrio-Hernandez, D. Memon, C. Hernandez-Armenta, J. Lyu, C.J.P. Mathy, T. Perica, K.B. Pilla, S.J. Ganesan, D.J. Saltzberg, R. Rakesh, X. Liu, S.B. Rosenthal, L. Calviello, S. Venkataramanan, J. Liboy-Lugo, Y. Lin, X.-P. Huang, Y. Liu, S. A. Wankowicz, M. Bohn, M. Safari, F.S. Ugur, C. Koh, N.S. Savar, Q.D. Tran, D. Shengjuler, S.J. Fletcher, M.C. O'Neal, Y. Cai, J.C.J. Chang, D.J. Broadhurst, S. Klippsten, P.P. Sharp, N.A. Wenzell, D. Kuzuoglu-Ozturk, H.-Y. Wang, R. Trenker, J.M. Young, D.A. Cavero, J. Hiatt, T.L. Roth, U. Rathore, A. Subramanian, J. Noack, M. Hubert, R.M. Stroud, A.D. Frankel, O.S. Rosenberg, K.A. Verba, D.A. Agard, M. Ott, M. Emerman, N. Jura, M. von Zastrow, E. Verdin, A. Ashworth, O. Schwartz, C. d'Enfert, S. Mukherjee, M. Jacobson, H.S. Malik, D.G. Fujimori, T. Ideker, C.S. Craik, S.N. Floor, J.S. Fraser, J.D. Gross, A. Sali, B.L. Roth, D. Ruggero, J. Taunton, T. Kortemme, P. Beltrao, M. Vignuzzi, A. García-Sastre, K.M. Shokat, B.K. Shoichet, N.J. Krogan, A SARS-CoV-2 protein interaction map reveals targets for drug repurposing, Nature 583 (2020) 459–468, https://doi.org/10.1038/s41586-020-2286-9.
[33] X. Hu, Z. Zhou, F. Li, Y. Xiao, Z. Wang, J. Xu, F. Dong, H. Zheng, R. Yu, The study of antiviral drugs targeting SARS-CoV-2 nucleocapsid and spike proteins through large-scale compound repurposing, Heliyon 7 (2021), https://doi.org/10.1016/J.HELIYON.2021.E06387.
[34] E. Furuta, K. Yamamoto, D. Tatebe, K. Watabe, T. Kitayama, R. Utsumi, Targeting protein homodimerization: a novel drug discovery system, FEBS Lett. 579 (2005) 2065–2070, https://doi.org/10.1016/J.FEBSLET.2005.02.056.
[35] A. Okada, Y. Gotoh, T. Watanabe, E. Furuta, K. Yamamoto, R. Utsumi, Targeting two-component signal transduction: a novel drug discovery system, Methods Enzymol. 422 (2007) 386–395, https://doi.org/10.1016/S0076-6879(06)22019-6.
[36] C. Chang, R.C. Stewart, The two-component SystemRegulation of diverse signaling pathways in prokaryotes and eukaryotes, Plant Physiol. 117 (1998) 723–731, https://doi.org/10.1104/PP.117.3.723.
[37] M. Rahmita, Pengembangan Sistem Penapisan Obat Antituberkulosis Baru Dengan Target PhoR Mycobacterium tuberculosis H37Rv Menggunakan Protein Represor AraC Escherichia coli, Bandung Institute of Technology, School of Life Sciences and Technology, 2015.
[38] A. Fibriani, Feraliana, N. Steven, M. Rahmita, E.A. Giri-Rachman, Plasmid construction for development of a high throughput system selection of new anti-HIV drugs derived from biological resources Indonesia, Biotechnol Ind J 14 (2018) 166.
[39] K.P. Sukma, P.C. Destiani, A. Fibriani, Implementation of dimer-based screening system in Escherichia coli BL21(DE3) for selection of actinomycetes compounds as anti-HIV candidate, HAYATI J. Biosci. 29 (2022) 192–203, https://doi.org/10.4308/HJB.29.2.192-203.
[40] E.A. Giri-Rachman, A. Fibriani, A.A.P. Taharuddin, M.H.S. Azmi, Plasmid Vektor Ekspresi Rekombinan Untuk Penapisan Cepat Kandidat Obat Anti-SARS-CoV-2 Yang Menarget Sisi Dimerisasi Dari Protomer Main Protease SARS-CoV-2, 2021, P00202110062.
[41] K. Gangavarapu, A.A. Latif, J.L. Mullen, M. Alkuzweny, E. Hufbauer, G. Tsueng, E. Haag, M. Zeller, C.M. Aceves, K. Zaiets, M. Cano, X. Zhou, Z. Qian, R. Sattler, N.L. Matteson, J.I. Levy, R.T.C. Lee, L. Freitas, S. Maurer-Stroh, M.A. Suchard, C. Wu, A.I. Su, K.G. Andersen, L.D. Hughes, Outbreak.info genomic reports: scalable and dynamic surveillance of SARS-CoV-2 variants and mutations, Nat. Methods 2023 (20) (2023 204) 512–522, https://doi.org/10.1038/s41592-023-01769-3.
[42] V.M. Kumbar, U. Muddapur, A. Bin Muhsinah, S.A. Alshehri, M.M. Alshahrani, I.A. Almazni, M.S. Kugaji, K. Bhat, M.R. Peram, M.H. Mahnashi, S.J. Nadaf, S. B. Rooge, A.A. Khan, I.A. Shaikh, Curcumin-encapsulated nanomicelles improve cellular uptake and cytotoxicity in cisplatin-resistant human oral cancer cells, J. Funct. Biomater. 13 (2022) 158, https://doi.org/10.3390/JFB13040158, 2022, 13, 158.
[43] G.N. Zirihi, L. Mambu, F. Guédé-Guina, B. Bodo, P. Grellier, In vitro antiplasmodial activity and cytotoxicity of 33 West African plants used for treatment of malaria, J. Ethnopharmacol. 98 (2005) 281–285, https://doi.org/10.1016/J.JEP.2005.01.004.
[44] M.H. Khosropanah, A. Dinarvand, A. Nezhadhosseini, A. Haghighi, S. Hashemi, F. Nirouzad, S. Khatamsaz, M. Entezari, M. Hashemi, H. Dehghani, Analysis of the antiproliferative effects of curcumin and nanocurcumin in MDA-mb231 as a breast cancer cell line, Iran. J. Pharm. Res. IJPR. 15 (2016) 231. /pmc/articles/PMC4986125/. (Accessed 8 April 2023).
[45] M. Wang, R. Cao, L. Zhang, X. Yang, J. Liu, M. Xu, Z. Shi, Z. Hu, W. Zhong, G. Xiao, Remdesivir and chloroquine effectively inhibit the recently emerged novel coronavirus (2019-nCoV) in vitro, Cell Res. (30) (2020) 269–271, https://doi.org/10.1038/s41422-020-0282-0, 2020 303.
[46] MedChemExpress. Remdesivir (Synonyms: GS-5734), 2023. https://www.medchemexpress.com/Remdesivir.html. (Accessed 16 July 2023).
[47] L. Zhang, J. Liu, R. Cao, M. Xu, Y. Wu, W. Shang, X. Wang, H. Zhang, X. Jiang, Y. Sun, H. Hu, Y. Li, G. Zou, M. Zhang, L. Zhao, W. Li, X. Guo, X. Zhuang, X. Lou Yang, Z.L. Shi, F. Deng, Z. Hu, G. Xiao, M. Wang, W. Zhong, Comparative antiviral efficacy of viral protease inhibitors against the novel SARS-CoV-2 in vitro, Virol. Sin. 35 (2020) 776, https://doi.org/10.1007/S12250-020-00288-1.
[48] H. Hu, M.D. Mady Traore, R. Li, H. Yuan, M. He, B. Wen, W. Gao, C.B. Jonsson, E.A. Fitzpatrick, D. Sun, Optimization of the prodrug moiety of remdesivir to improve lung exposure/selectivity and enhance anti-SARS-CoV-2 activity, J. Med. Chem. 65 (2022) 12044–12054, https://doi.org/10.1021/ACS.JMEDCHEM.2C00758.
[49] Selleck Chemicals. Ritonavir (ABT-538) (Catalog No.S1185) (Synonyms: ABT-538,A 84538, RTV, Norvir, Norvir Softgel), 2023. https://www.selleckchem.com/products/Ritonavir.html. (Accessed 16 July 2023).
[50] J.S. Fridman, P.A. Scherle, R. Collins, T.C. Burn, Y. Li, J. Li, M.B. Covington, B. Thomas, P. Collier, M.F. Favata, X. Wen, J. Shi, R. McGee, P.J. Haley, S. Shepard, J.D. Rodgers, S. Yeleswaram, G. Hollis, R.C. Newton, B. Metcalf, S.M. Friedman, K. Vaddi, Selective inhibition of JAK1 and JAK2 is efficacious in rodent models of arthritis: preclinical characterization of INCB028050, J. Immunol. 184 (2010) 5298–5307, https://doi.org/10.4049/JIMMUNOL.0902819.
[51] Selleck Chemicals. Baricitinib (Catalog No.S2851) (Synonyms: INCB028050, LY3009104), 2023. https://www.selleckchem.com/products/baricitinib-ly3009104.html. (Accessed 16 July 2023).